# Experimental Evaluation of the Effect of Temperature on the Mechanical Properties of Setting Materials for Well Integrity

**Adijat Ogienagbon[1]* and Mahmoud Khalifeh[1]**

[1]Department of Energy and Petroleum Engineering, University of Stavanger, Norway

## Summary

A fundamental understanding of the mechanical properties of zonal isolation materials is important for predicting well integrity during well operation conditions. Conventionally, the mechanical properties of zonal isolation materials are tested at ambient temperature using uniaxial testing. This study examined the mechanical properties of alternative zonal isolation materials such as rock-based geopolymer, thermosetting resin, and an industrial class expansive cement under realistic well conditions by triaxial testing. Mechanical properties such as Young's modulus, Poisson's ratio, cohesive strength, friction angle, and compressive strength of these materials at 30 and 90°C were compared. The effect of confining pressure on the mechanical properties of the materials was also examined. The findings of this study show that all selected materials possess compressive strength at 30 and 90°C and that the compressive strength of all the selected materials is strongly impacted by temperature and confining pressure. The Young's modulus of all the selected materials was unaffected by confining pressure, while only the Young's modulus of thermosetting resin was sensitive to temperature. The influence of temperature on the Poisson's ratio varied from one material to another. In addition, when the test temperature increased, the friction angle of neat Class G and geopolymer decreased.

## Introduction

Over four million onshore hydrocarbon wells have been drilled in various locations globally (Davies et al. 2014). On the Norwegian Continental Shelf alone, it is reported that around 7,200 offshore wells have been drilled as of August 2021. Nearly 4,000 of these wells have been permanently plugged and abandoned (Norwegian Petroleum Directorate 2021). It is crucial that the integrity of all subsurface boreholes be maintained regardless of its stage in the life cycle, including post-abandonment. Loss of well integrity can lead to accidents, negative environmental impacts, loss of reserves, huge remediation costs because of expensive remedial treatment methods, or fatality. Significant well integrity issues have been documented in various locations around the world. Vignes (2011) reported that 75 of 406 wells suffered from well integrity issues on the Norwegian Continental Shelf, and of these, 28 were on shut-in status because of these issues. An extensive review of different types of wells around the world was carried out by Davies et al. (2014). They examined several data sets of wells varying in age, designs, and the number of wells and reported that the number of wells suffering from well integrity issues ranged between 1.9 and 75% depending on the data set considered. A study conducted on wells in the Gulf of Mexico revealed that around 33% of 6,650 wells suffering from well integrity are linked to cement failure. To prevent the undesirable consequences of unwanted fluid migration, optimum zonal isolation elements must be put in place. Several factors can contribute to the failure of zonal isolation materials and subsequent loss of hydraulic integrity. These factors include but are not limited to the presence of mudcake and poor cement displacement (Bois et al. 2012; Lecampion et al. 2013), axial and radial cement shrinkage (Sasaki et al. 2018), fluid loss (Nelson and Guillot 2006), and matrix permeability alteration (Bagheri et al. 2018). The geographical location, drilling environment, well design, and downhole conditions of wells are also essential parameters influencing well integrity (Kiran et al. 2017). In addition, thermal and mechanical stresses introduced to cement sheath are roots that can cause fluid migration through cement sheath (Zhang and Bachu 2011; Lavrov et al. 2015; Kjøller et al. 2016).

The Norwegian standard NORSOK D-010 (2021) is the widely used well integrity standard. This standard emphasizes the importance and guidelines for optimum zonal isolation, barrier materials, and well barrier envelopes. Portland cement has been traditionally used as a permanent isolation material to maintain well integrity and permanent plug and abandonment; this is mainly because of its known chemistry, initial low matrix permeability, relatively low price, commercial availability, availability of admixtures, and established reliability over time. However, complications with the short- and long-term use of cement have been reported by several researchers. These drawbacks include shrinkage, low ductility, instability at elevated temperature high-pressure conditions, instability in corrosive environments, and large carbon dioxide ($CO_2$) emission through its manufacturing (Geiker and Knudsen 1982; Shen et al. 2015; Sasaki et al. 2018; Vrålstad et al. 2019a).

Cement defects caused by mechanical stresses can serve as a conduit for the migration of formation fluids. It is important to highlight the distinction between mechanical and hydraulic integrity of zonal isolation materials (Bois et al. 2011; Khalifeh and Saasen 2020; Kamali et al. 2021a). Where mechanical integrity implies the potential presence of cement defects, hydraulic integrity implies the resulting flow of fluids through the cement defect or around it. The development of plastic strain (i.e., irreversible strain because of plasticity) in zonal isolation materials is majorly responsible for the loss of their mechanical integrity. Improving the ductility of zonal isolation materials can help keep them within their elastic limits during the damaging influence of underground mechanical stresses, thereby prolonging the long-term hydraulic integrity of the zonal isolation materials. A fundamental understanding of the mechanical properties of

*Corresponding author; email: adijat.a.ogienagbon@uis.no



Original SPE manuscript received for review 8 November 2021. Revised manuscript received for review 24 January 2022. Paper (SPE 209794) peer approved 28 February 2022.

the complete well system, which includes the steel casing, cement, and rock under realistic borehole conditions, is important for safe and long-lasting well design (Thiercelin et al. 1998; De Andrade et al. 2016). Boukhelifa et al. (2004) performed mechanical and zonal isolation tests on seven cement systems with varying mechanical properties. They reported that mechanical properties such as elasticity, strength, and expansion were vital for maintaining cement integrity, confirming the experimental findings of Le Roy-Delage et al. (2000). Wu and Salehi (2020) showed that the casing-cement interface is the weak point under diametric compression load and more susceptible to failure than the cement-formation interface.

The experimental methods for determining the mechanical properties of cement are described by industry standards such as the American Society for Testing and Materials (ASTM 2012) and American Petroleum Institute (API RP 10B-2 2013). A competent barrier element should be impermeable, resist corrosion of underground fluids, nonshrinking, and withstand thermal and mechanical stress encountered in the wellbore. Over the past years, researchers have proposed alternative materials to Portland cement. While some of these materials are currently being used, others are still emerging. These include geopolymers (i.e., inorganic polymers known as artificial rocks), organic polymer resins, expansive cement, blast furnace slag, bentonite, metal alloys, unconsolidated sand slurries, and thermite-based (Beharie et al. 2015; Jafariesfad et al. 2017b; Khalifeh et al. 2018; Vrålstad et al. 2019a).

Most researchers measure the mechanical properties of the materials by uniaxial testing at ambient conditions. This study compares the mechanical properties of three of these alternative zonal isolation materials (geopolymer, expansive cement, and thermosetting resins) at 30 and 90°C using triaxial testing. The results will help improve understanding of the performance of zonal isolation materials under varying temperature conditions encountered downhole. In addition, we compared the performance of these materials. Mechanical properties such as confined compressive strength, Young's modulus, and Poisson's ratio of the materials were compared with a reference case of Class G cement at both low and elevated temperatures. The results were also compared with those reported in an earlier publication using the uniaxial testing procedure to evaluate the effect of confining pressure on the measured mechanical properties (Kamali et al. 2021b). These measured mechanical properties can be used as a database for modeling by other researchers.

## Materials

**Portland Cement.** Portland cement is the most commonly used cementitious material. It is manufactured by grinding clinker produced from the cement kiln, which mainly consists of hydraulic silicates, calcium aluminates, and aluminoferrites (Nelson and Guillot 2006). Produced cement is graded into different classes from A to H. Their classification is based on their level of reactivity, composition, particle-size distribution, temperature, resistivity to chemicals, and depth of placement. Class G and Class H are the most used cement classes today in the oil and gas industry. Both Class G and Class H share similar chemical composition; however, Class G cement is more finely ground than Class H. Neat Class G cement without any additives was used in this study as reference.

**Industrial Expansive Cement.** Shrinkage is one of the major concerns associated with the hydraulic sealability performance of cementitious materials, especially ordinary Portland cement. The hydration reaction of cement can result in restrained volumetric shrinkage of cement (Kamali et al. 2021b), which could have detrimental effects on the cement's mechanical properties and sealing capacity. The use of expanding agents such as magnesium oxide (MgO), calcium oxide (CaO), superabsorbent polymers, and saturated aggregates can help mitigate the effects of shrinkage and inherent debonding of cement at the interface (Jafariesfad et al. 2017c; Saito et al. 1991; Mo et al. 2014). The successful use of MgO as an expansive agent in cement has been acknowledged by several researchers (Mo et al. 2012; Sherir et al. 2017) who have reported the self-healing ability of the MgO-enhanced cement systems. To produce sound cement for use in real well operations, the recommended volume of MgO should be limited to $\leq$6% (ASTM 2001).

**Thermosetting Resin.** Thermosetting polymer (resins) are particle-free, liquid barrier materials whose curing processes are activated with temperature. This material is an organic polymer with the possibility of adjusting its pumping time and setting time to suit specific borehole temperatures. In addition, the density and viscosity of thermosetting resins can be tailored to improve their pumpability. Resins have been used in various locations for plugging and remedial operations (Al-Ansari et al. 2015; Davis 2017). Although their usage as zonal isolation material and abandonment material has been limited, they are a good candidate for remedial jobs because of their low viscosity profile. The mechanical properties of resins have been reported to outperform that of cement, although a considerable loss of compressive and flexural strength was detected when exposed to corrosive environments like crude oil (Beharie et al. 2015).

**Geopolymer.** Geopolymers are inorganic polymers made from different types of raw materials, which have favorable aluminosilicate content and morphology. They are formed from an aluminosilicate-rich solid-phase reaction (typically blast furnace slag, fly ash, naturally occurring rocks, or thermally activated clay) and a hardener phase (e.g., alkali silicate solution, alkali solution, or a combination of both). Geopolymer provides an environmentally friendly alternative to cement with an 80% reduction in $CO_2$ production. Although the use of geopolymer in the construction industry is quite established, its potential for use in the oil and gas industry is currently being explored on a laboratory scale (Adjei et al. 2021; Khalifeh et al. 2015, 2018). Previous research on geopolymer had reported favorable mechanical properties, low permeability, and tolerance to contamination by formation fluids, suggesting its potential as a suitable barrier material for long-term well integrity (Salehi et al. 2018). The pumpability of geopolymer slurry mixes is sensitive to temperature, as higher temperatures can considerably lower pumping time (Salehi et al. 2018).

## Experimental Procedure

All the zonal isolation materials used in this study were prepared following the recommended recipes and procedures provided by the material suppliers. An in-depth description of the composition and specimen preparation is provided in Kamali et al. (2021b). All material slurries were conditioned at a bottomhole circulation temperature of 65°C. Slurries were then cured in cylindrical rubber sleeves at a bottomhole static temperature of 90°C and pressure of 17.2 MPa with access to water. The slurry preparation procedure for each material is described as follows:

- **Neat Class G Cement**: Class G cement from Dyckerhoff was used to prepare the slurry. The slurry was prepared with a water-cement ratio of 0.44 and mixed using a high-speed waring blender according to API RP 10B-2 (2013).
- **Industrial Class Expansive Cement**: MgO-enriched Class G cement was selected as the solid phase for the slurry. The slurry was prepared with water and other additives like microsilica, retarder, fluid loss controller, dispersant, and defoamer. The slurry was also mixed in accordance with API RP 10B-2 (2013) with a high-speed waring blender.

- **Geopolymer:** The precursor was mixed according to the recommended recipe. Active quenched blast furnace slag was added to naturally occurring aluminosilicate-rich rock to produce a normalized composition. A potassium silicate solution with a modular ratio of 2.49 was used as a hardener. The slurry was prepared in accordance with API RP 10B-2 (2013) using a high-speed waring blender.
- **Thermosetting Resin:** The thermosetting resin slurry was mixed according to the recommended procedure and composition provided by the supplier. Mixing was done for about 40 minutes using a Heidolph overhead stirrer at 600 rev/min. The thermosetting resin is composed of liquid resin, initiator, viscosifier, and filler to build the density of the slurry. It is important to note that the resin system used in this study is not a conventional particle-free system, as fillers have been added to build the density.

The samples were cured in autoclaves for 7 days at the defined downhole conditions. After curing, the autoclave was allowed to cool down and depressurized slowly to avoid thermal or pressure shocks in the specimens. The cooling and depressurization rates were selected in accordance with the API RP-10B-2 (2013) standard. The specimens were then taken out of the autoclaves and prepared for experiments. Before being loaded in the cell, the cylindrical core specimens were first shaped and cut to the desired dimensions (length ≥2 diameter) with a lathe and cutting machine. Both ends of the specimens were then ground to ensure smooth and even ends. The specimens were tested using an in-house triaxial test cell. All the materials were tested under the same conditions to ensure consistency, but it is acknowledged that the development of standards for characterizing the mechanical properties of thermosetting resins as barrier materials should be encouraged. The choice of neat G cement as reference material is not to qualify other materials as superior to it but to test a base case material that can be easily reproduced for testing.

**Triaxial Test.** The triaxial test was performed according to the recommended practice for testing the mechanical behavior of well cement (API TR 10TR7 2017). **Fig. 1** presents the experimental setup of the triaxial cell. The triaxial cell enabled the exertion of radial and axial stresses on the specimens simultaneously. The cell is connected to pumps, which are responsible for supplying stress to the system. The radial stress was provided by fluid pressure in the cell (in this case, oil pressure), while the axial stress was provided by a load piston situated at the top of the cell. The cell is equipped with an extensometer directly attached in the middle of the specimen to measure the radial deformation of the specimen. A linear variable differential transformer is installed at the top of the cell to measure the axial deformation of the specimen. Two types of tests were performed for each material, first at 30°C and another at 90°C, to represent an elevated well temperature condition. A heating jacket is wrapped around the triaxial cell to provide heating for tests carried out at 90°C. A minimum of three specimens were tested for each type of material at each test temperature to minimize the uncertainty in measurements. A confining pressure of 17.2 MPa and a monotonic loading rate of 35 MPa/min were applied during the test. The test is conducted in two stages. First, radial and axial stresses are simultaneously applied to reach a confining pressure of 17.2 MPa in the hydrostatic phase. After then, a maximum load of 45 MPa was monotonically loaded on the specimen in the deviatoric phase to mimic undrained test conditions. Although a recommended loading rate between 3.5 and 14 MPa/min is prescribed for monotonic loading of the specimens (API TR 10TR7 2017), a higher loading rate was selected in this study because of technical limitations; this can be assumed as a worst-case scenario where the material is exposed to a sudden pressure shock. This higher loading rate results in a 6% reduction in the compressive strength compared with those obtained from the recommended loading rate of 14 MPa/min (API TR 10TR7 2017).

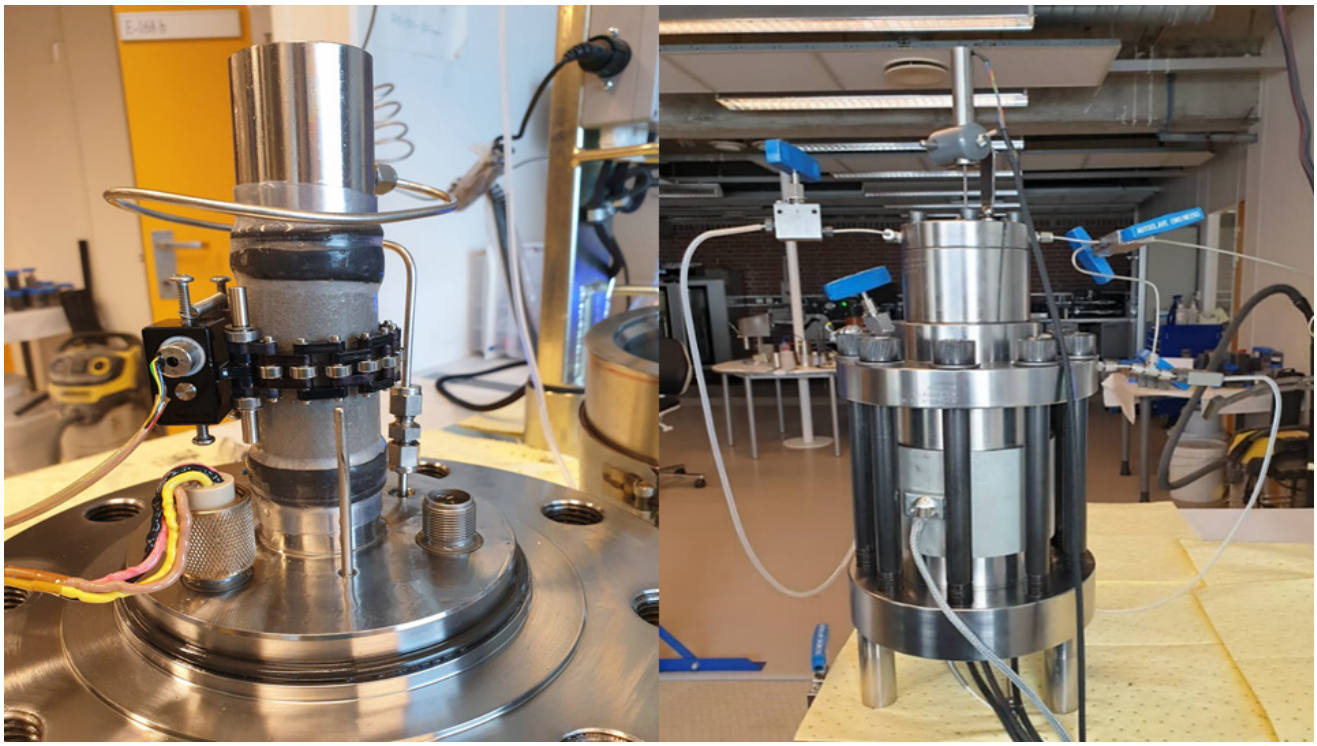

**Fig. 1—Setup of the triaxial cell.**

## Results and Discussion

**Young's Modulus.** Young's modulus is a measure of the stiffness of a material. In other words, it shows the capability of a material to be bent or stretched. It is calculated as the proportionality coefficient of the stress-strain curve at the elastic region. Materials with

low Young's modulus tend to be ductile, while materials with high Young's modulus tend to be brittle. The Young's modulus of a zonal isolation material is crucial to its resistance of deformation when it encounters mechanical stresses downhole. This is especially because cement is typically susceptible to failure than casing when subjected to mechanical stresses (Vrålstad et al. 2019b). Therefore, the compatibility of the mechanical properties of zonal isolation material with surrounding casing and formation has been outlined (Bois et al. 2012; Salehi et al. 2018). Studies have also shown that the compressive strength to Young's modulus ratio and tensile strength to Young's modulus ratio are more critical to zonal isolation than their individual parameters (Jafariesfad et al. 2017a; Kamali et al. 2021b). The stress-strain curves of the candidate materials at 30°C are presented in **Fig. 2.** The Young's modulus of the candidate materials was calculated through linear regression of the elastic region of the stress-strain curve during deviatoric loading, as presented in **Fig. 2**. The results from the axial stress-strain curve show that expansive cement has the highest Young's modulus. It is closely followed by the neat G cement, thermosetting resin, and geopolymer, which had the lowest Young's modulus. Geopolymer was observed to experience considerable creeping with a large strain of about 0.034 before failure compared with the other materials at 30°C.

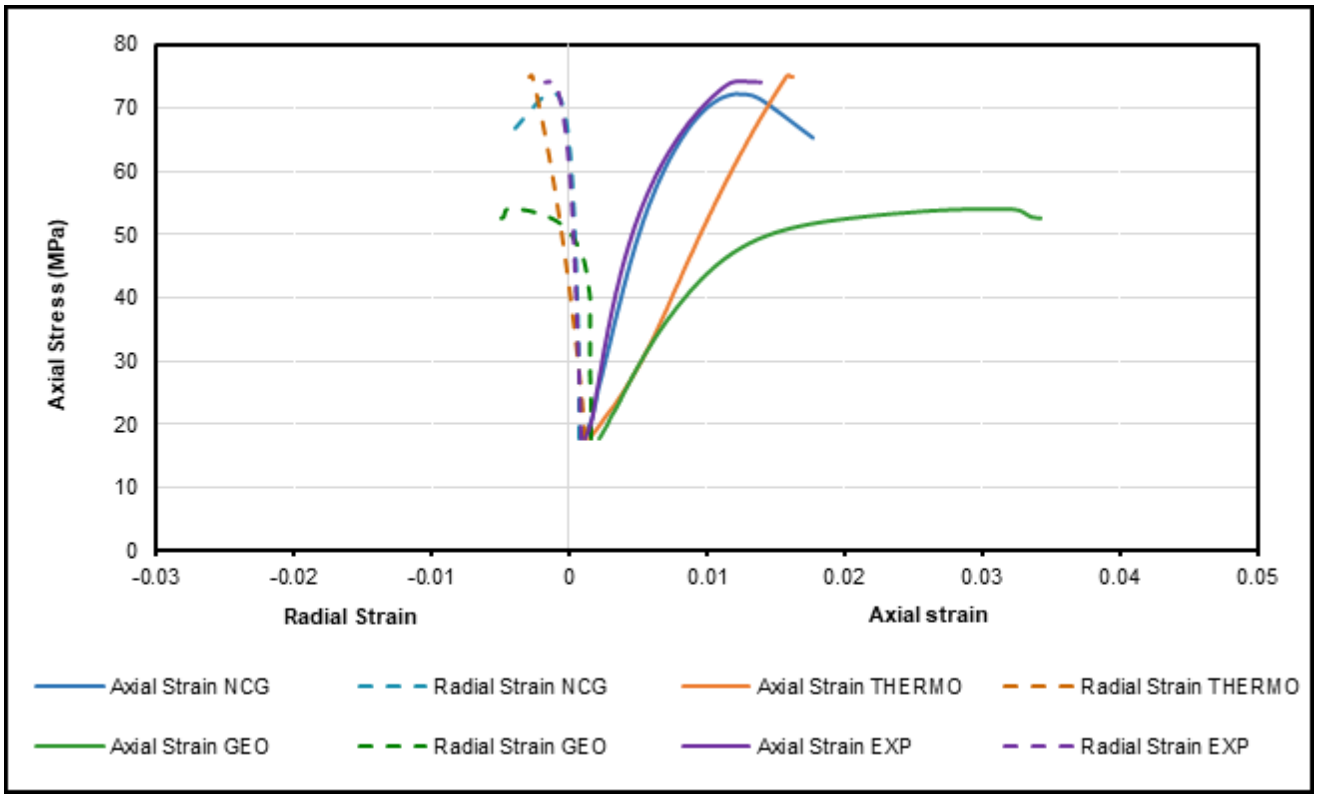


**Fig. 2—Stress-strain curves of selected zonal isolation materials at 30°C (maximum loading limit of 74 MPa).**

The large strain bearing capacity of geopolymers during axial compression is also reported in Kimanzi et al. (2020). The ductility of Class G cement observed in the stress-strain curves presented in **Fig. 2** is consistent with the findings of Chen and Xu (2018), where they found that cement exhibited ductile behavior when the confining pressure is higher than 15 MPa. **Fig. 3** presents the stress-strain curves of the candidate materials at 90°C. It is seen that the order of stiffness amongst the zonal isolation materials is the same as that at 30°C. Expansive cement still retained the highest Young's modulus, followed by the neat G cement, thermosetting resin, and lastly, geopolymer. A significant increase in ductility was observed for the thermosetting resin when tested at 90°C, while temperature did not significantly impact the creep of geopolymers. The effect of temperature on the calculated average Young's modulus of the selected materials is presented in **Fig. 4.** It is seen that an increase in temperature did not significantly impact the Young's modulus of the zonal isolation materials except for thermosetting resin. This is comparable to results reported for neat G cement by Zheng et al. (2017). At 30°C, the average Young's modulus of thermosetting resin was 5.7 GPa. However, with increasing temperature, the average Young's modulus of thermosetting resin decreased to 1.8 GPa. This indicates a strong sensitivity of the stiffness of thermosetting resin to temperature because they are organic components whose long chains are temperature-dependent (Van den Ende et al. 2007). Geopolymer exhibited a low Young's modulus of 4 GPa compared with the other materials at 30°C and retained its flexibility at 90°C with a Young's modulus of 3.5 GPa (Khalifeh et al. 2015); this is believed to be rooted in its inorganic polymer sizes. Expansive cement showed the highest Young's modulus of all the candidate materials at 30°C and became slightly stiffer with increased temperature. The increase in its Young's modulus with temperature is consistent with the reduction ductility observed in the stress-strain curves in **Fig. 3**. Zonal isolation materials with a low Young's modulus are less susceptible to failure (Le Roy-Delage et al. 2000; Therond et al. 2017). Therefore, the lower Young's modulus of geopolymers and thermosetting resins may improve their ability to maintain zonal isolation at low and elevated temperatures.

**Poisson's Ratio.** Poisson's ratio (V) is the measure of deformation in the material in a direction perpendicular to the direction of compression. It is defined as the ratio of radial strain to axial strain. The Poisson's ratio was determined similarly to the Young's modulus but from the radial strain-axial strain ($\mathcal{E}_r$-$\mathcal{E}_a$) curve. The linear regression analyses for both Poisson's ratio and Young's modulus should be obtained from the same range. All the selected materials presented an increase in Poisson's ratio when the temperature was increased (see **Fig. 5**). Both thermosetting resin and geopolymer were most sensitive to temperature. When the temperature was increased, the radial strain of both materials increased considerably (see **Fig. 3**), leading to an increase in the Poisson's ratio. The Poisson's ratio of

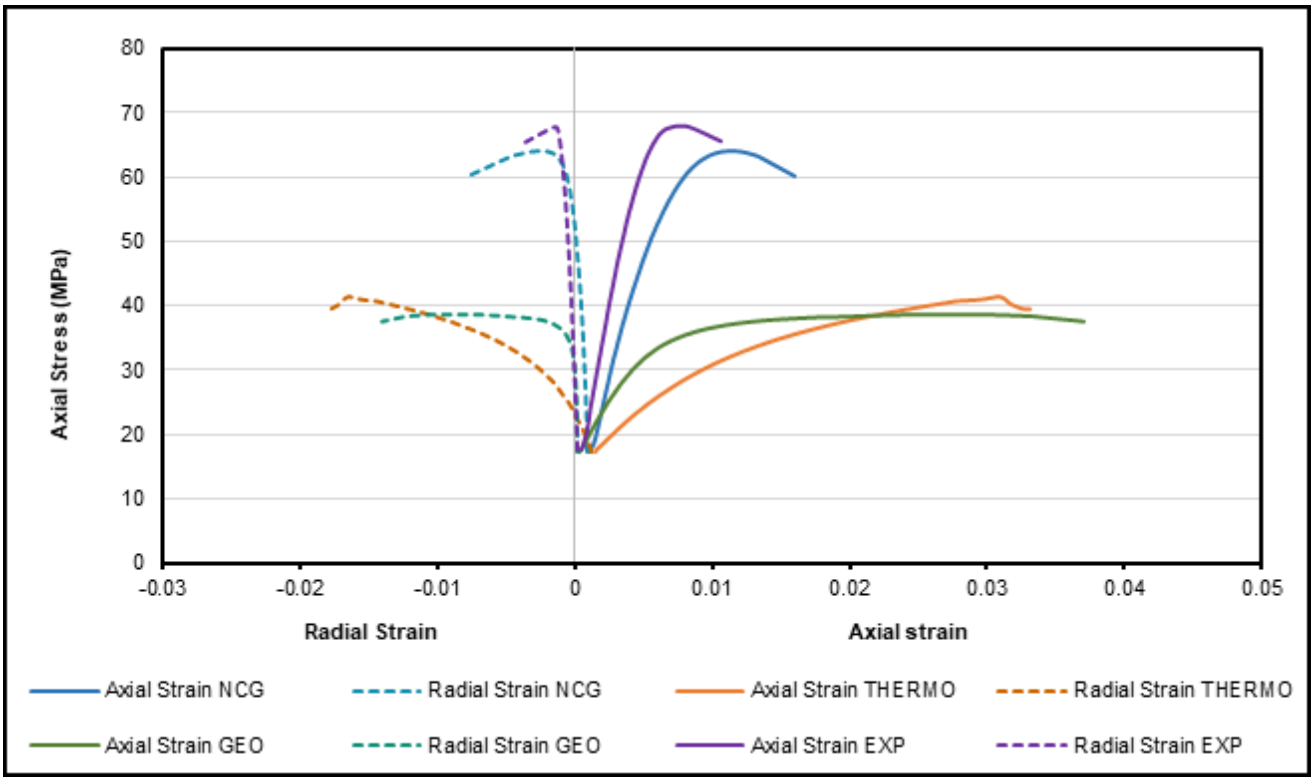


**Fig. 3—Stress-strain curves of selected zonal isolation materials at 90°C (maximum loading limit of 74 MPa).**

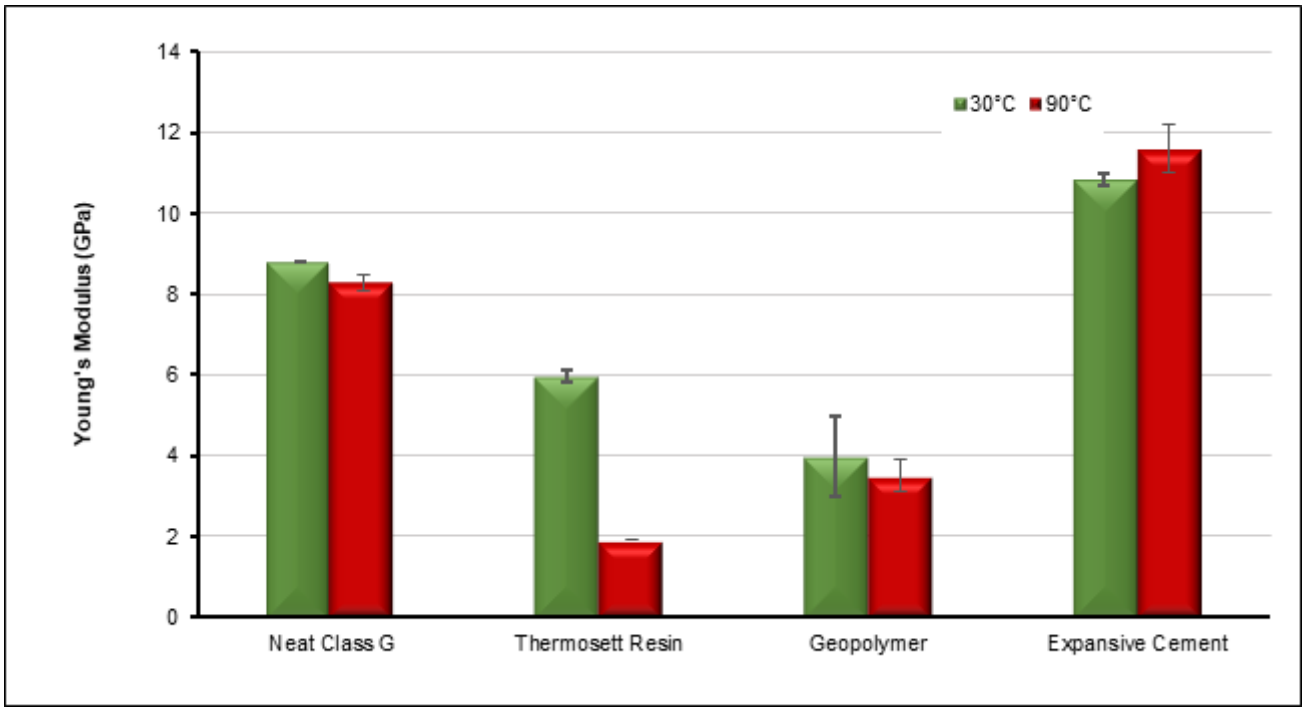


**Fig. 4—Effect of temperature on the average Young's modulus of selected zonal isolation materials.**

thermosetting resin and geopolymer at 30°C is 0.28 and 0.19, respectively. At 90°C, the Poisson's ratio of thermosetting resin increased to 0.45, while that of geopolymer increased to 0.30. Neat G cement experienced an increase in Poisson's ratio with temperature from 0.09 to 0.16, and expansive cement only increased from 0.17 to 0.19. Increasing the Poisson's ratio of a zonal isolation material will decrease the magnitude of the destructive hoop and shear stresses induced in the material, thereby reducing the risk of failure (Kwatia et al. 2017). Therefore, a material with a relatively higher Poisson's ratio may exhibit long-term integrity over a material with a low Poisson's ratio (Therond et al. 2017). The increase in flexibility of the zonal isolation materials at 90°C may imply that they may be able to withstand more deformation at elevated temperatures.

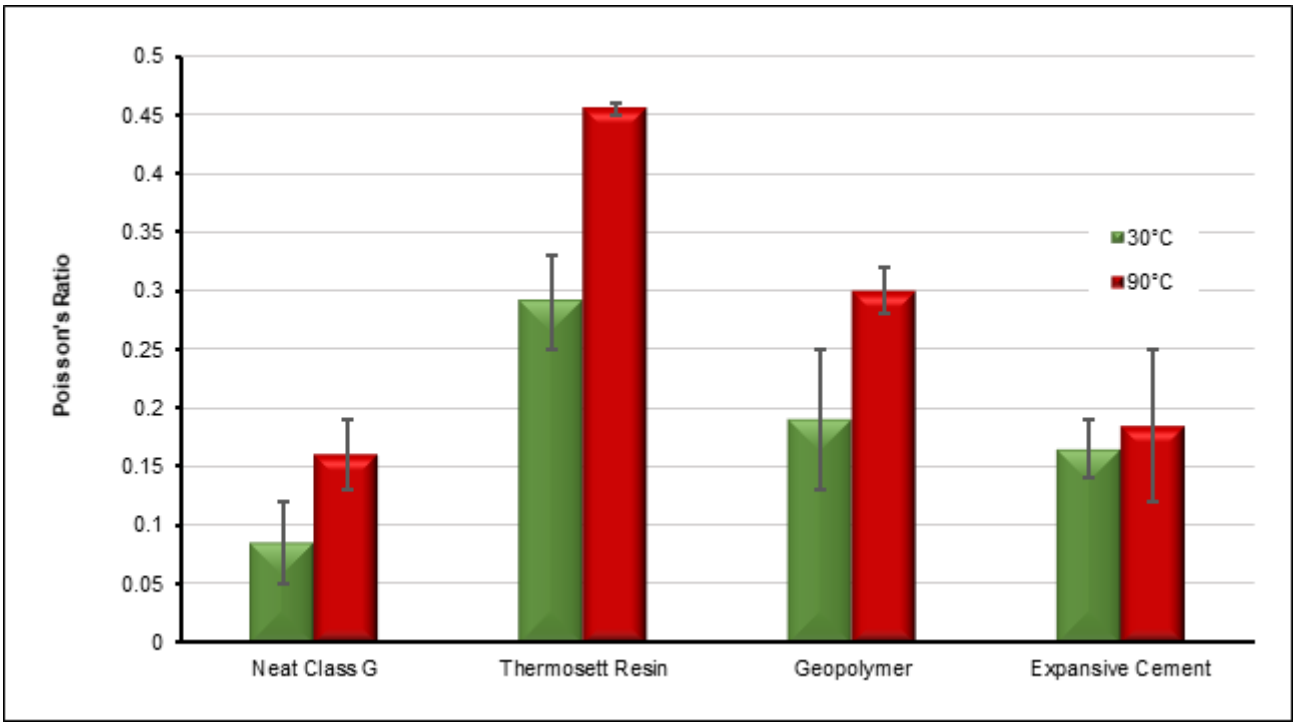


**Fig. 5—Effect of temperature on the average Poisson's ratio of selected zonal isolation materials.**

**Confined Compressive Strength.** Conventionally, the unconfined compressive strength of cement can be estimated during uniaxial testing or by an ultrasonic cement analyzer. During triaxial testing, the confined compressive strength of the zonal isolation materials can be estimated similarly to that of the unconfined compressive strength from the stress-strain curves. The maximum stress the specimen can withstand before entering plastic failure is defined as the confined compressive strength (API TR 10TR7 2017). The test temperature seems to play an important role in the confined compressive strength of the specimen, as seen in **Fig. 6.** All the tested materials experienced failure at 90°C, but only geopolymer and Class G cement experienced failure at 30°C. The compressive strength of thermosetting resin and expansive cement could not be estimated at 30°C because the specimens did not fail within the maximum loading limits of this test (74 MPa).

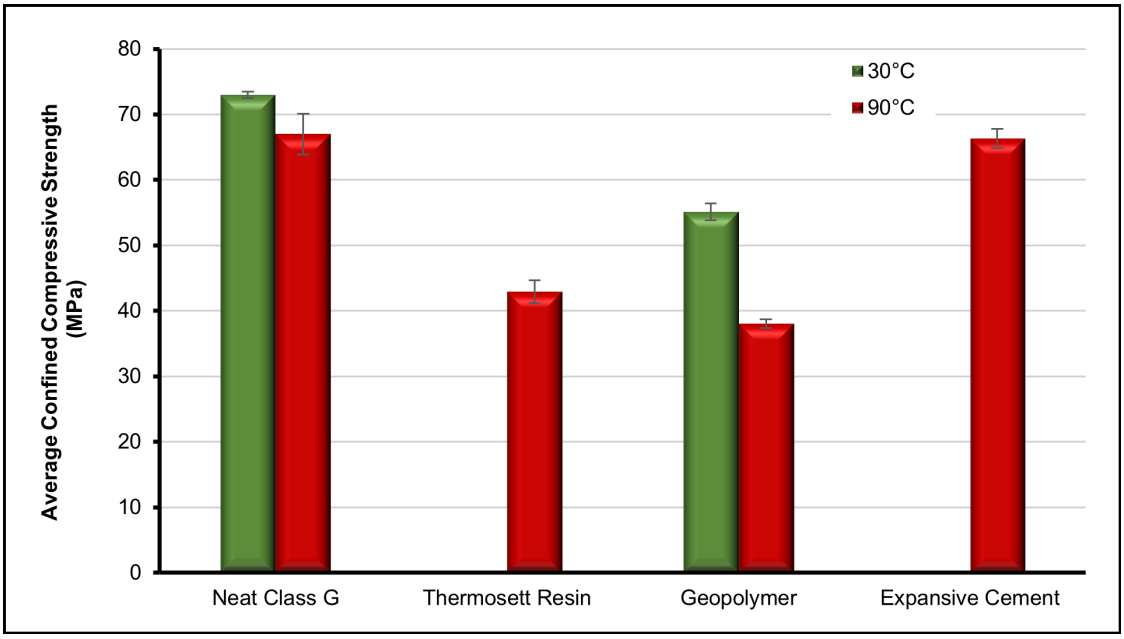


**Fig. 6—Effect of temperature on the average confined compressive strength of selected zonal isolation materials.**

It can be seen in **Fig. 2** that the stress-strain curves for both specimens did not show a dip in axial stress before reaching 74 MPa. On the contrary, a short plateau can be seen at the maximum loading limit before the experiment is stopped and axial stress starts to dip. **Fig. 7** presents some samples of the selected materials after testing at 30°C. Thermosetting resin and expansive cement did not show any visible

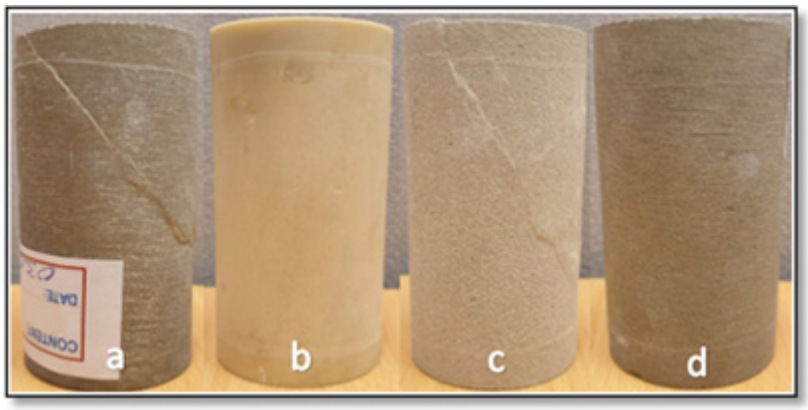


**Fig. 7—Selected specimens after testing at 30°C: (a) Class G cement with shear failure; (b) thermosetting resin without failure; (c) geopolymer with shear failure; and (d) expansive cement without failure.**

failure after testing at 30°C; this implies that the compressive strength of thermosetting resin and expansive cement is higher than that of Class G cement and geopolymer at 30°C. **Fig. 8** provides the failure patterns of the selected candidate materials after testing at 90°C. Despite the observation of failure in the stress-strain curves of thermosetting resin during deviatoric loading at 90°C, there was no visible fracture on the specimens upon close inspection after the test. The samples, however, appeared to have barrelled by undergoing considerable radial expansion and length shortening. Further inspection was carried out by slicing the specimen to investigate the presence of internal cracks on the specimen (see **Fig. 8**), yet no visible cracks or defects were observed. The absence of visible cracks on the thermosetting resin specimens may be because of the self-healing ability of the resins to close initiated cracks as temperature decreased after the test. The measurements revealed that though the curing conditions of the samples are the same, increasing testing temperature from 30 to 90°C caused the reduction of the compressive strength of all the materials studied. The average compressive strength of neat G cement reduced from 72 to 67 MPa, while that of geopolymer reduced from 55 to 38 MPa. Increasing the compressive strength of a zonal isolation material reduces its risk of damage (Therond et al. 2017). At both 30 and 90°C, expansive cement and neat G cement showed high confined compressive strength; therefore, both zonal isolation materials may be considered in low and elevated-temperature applications where a material with a high compressive strength is preferred.

**Confined Compressive Strength to Young's Modulus.** The compressive strength and Young's modulus of zonal isolation materials are two major important mechanical parameters that influence the mechanical integrity of the materials. While compressive strength is an indicator of maximum cement strength, the Young's modulus is an indicator of the material's flexibility. A good zonal isolation material should possess a high compressive strength and a low Young's modulus (Jafariesfad et al. 2017a). To evaluate which of these materials possesses the best of both properties, the ratio of the compressive strength to Young's modulus is estimated at both temperatures and presented in **Fig. 9.** The measurements show that despite the lower compressive strength of geopolymer compared with the other materials at both temperatures, it retains a high potential to maintain zonal isolation because of its lower Young's modulus. This same characteristic is reported for thermosetting resin at 90°C. Although expansive cement possesses a high compressive strength, its high stiffness may influence its zonal isolation potential.

**Effect of Confining Pressure on Young's Modulus and Compressive Strength.** In a confined triaxial test, each side of the specimen is subjected to a known confining stress, while in the unconfined condition, the specimen is unrestrained at the sides and allowed to bulge out freely during loading. Kamali et al. (2021b) conducted uniaxial testing of the selected zonal isolation materials. The material preparation procedure and test parameters used in that study were similar to those used in this study. Therefore, a comparison was conducted between the results obtained in this study at 30°C and those obtained in Kamali et al. (2021b). The effect of confining pressure on the average values of Young's modulus and compressive strength of the materials is presented in **Figs. 10 and 11**, respectively. It is seen in **Fig. 10** that the Young's modulus of the zonal isolation materials is insensitive to confining pressure. The Youngs modulus of all the selected materials was quite similar for the unconfined case reported in Kamali et al. (2021b) and confined case reported in this study. This finding is consistent with reported literature (API TR 10TR7 2017; Thiercelin et al. 1998). The confined compressive strength of thermosetting resin and expansive cement was higher than the maximum load applied during this test. However, a comparison was made for Class G and geopolymer. A strong influence of confining pressure is observed on the compressive strength of Class G and geopolymer. Both materials exhibit higher compressive strength when tested under confining pressure. Nevertheless, Class G has a higher compressive strength overall. When comparing the magnitude of influence of confining pressure on both materials, geopolymer Class G experienced an 82% increase, while geopolymer experienced an increase of more than 300% in its compressive strength because of confining pressure. Therefore, an increase in confining pressure leads to an increase in the compressive strength of zonal isolation materials (API TR 10TR7 2017; Chen and Xu 2018).

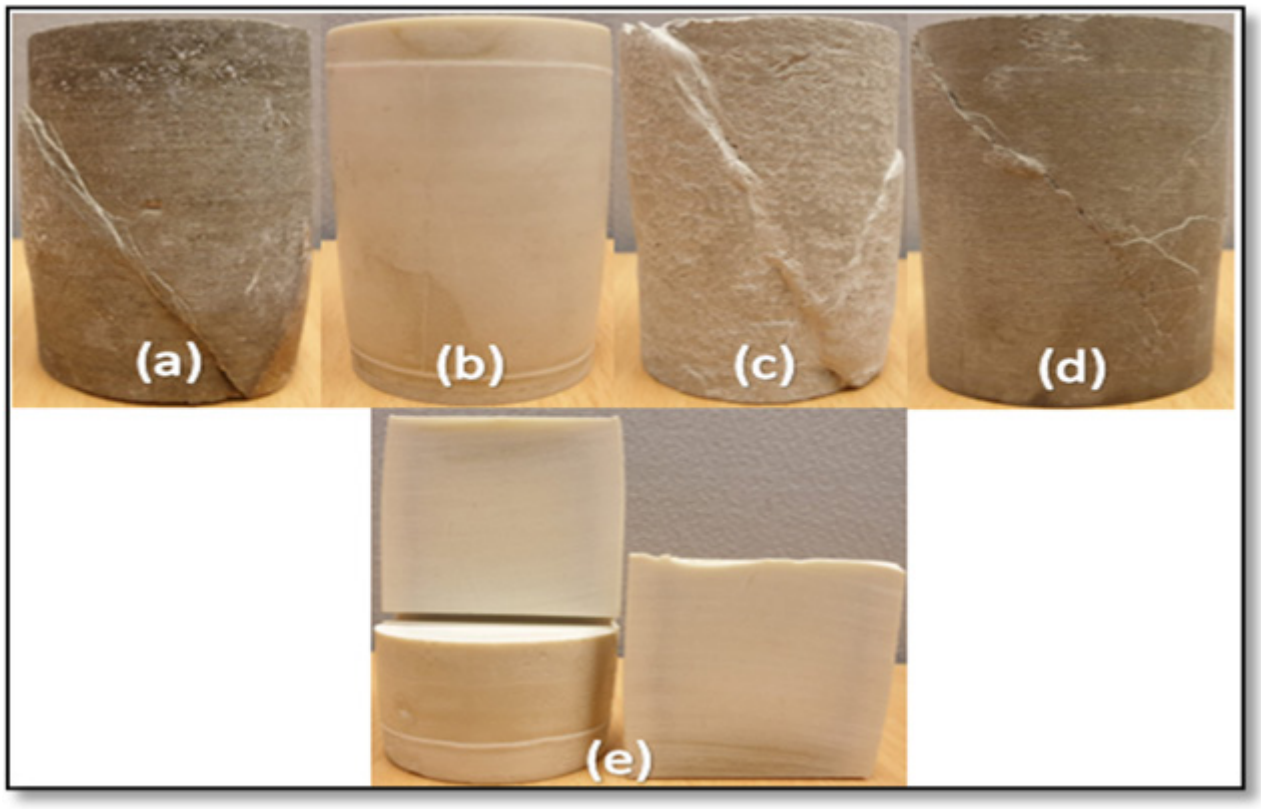


**Fig. 8—Selected specimens after testing at 90°C: (a) Class G cement with shear failure; (b) barrelled thermosetting resin; (c) geopolymer with shear failure; (d) expansive cement; and (e) sliced thermosetting resin specimen without any cracks.**

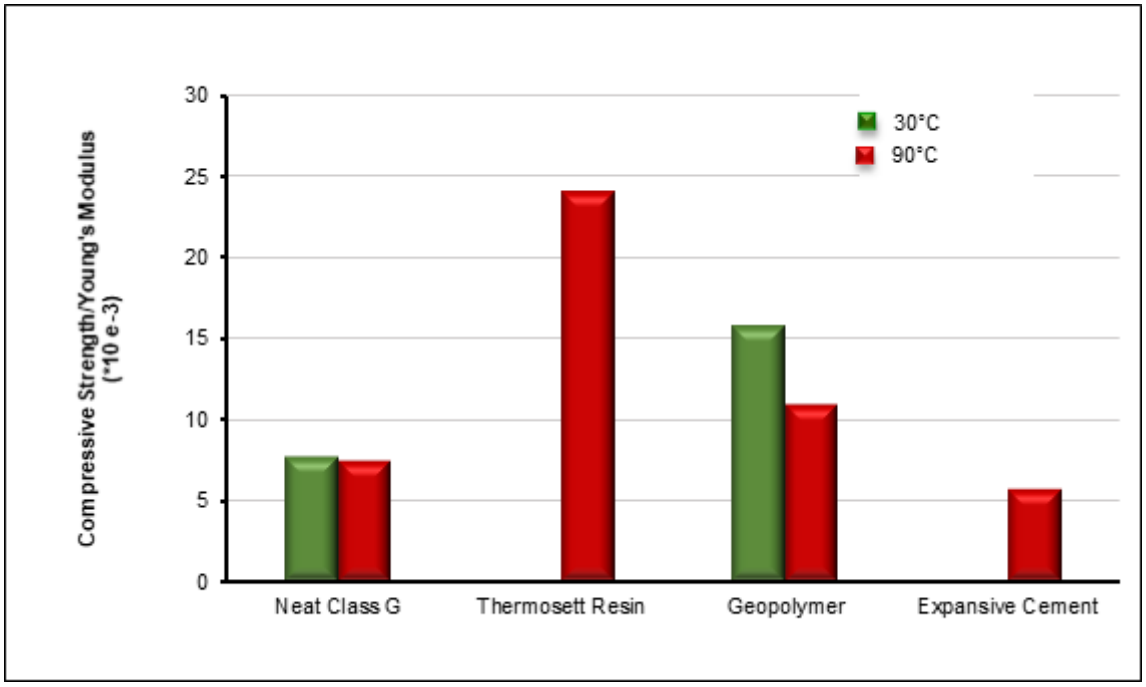


**Fig. 9—Effect of temperature on the confined compressive strength/Young's modulus of selected zonal isolation materials.**

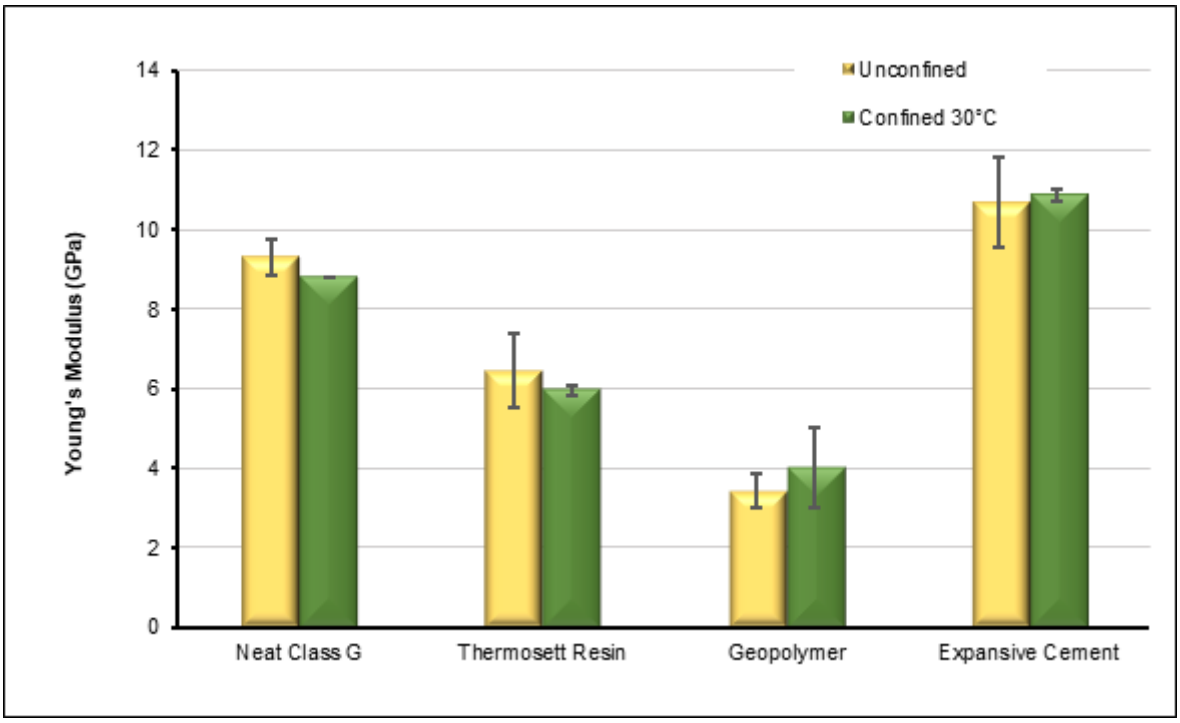


**Fig. 10—Effect of confining pressure on the average Young's modulus of selected zonal isolation materials.**

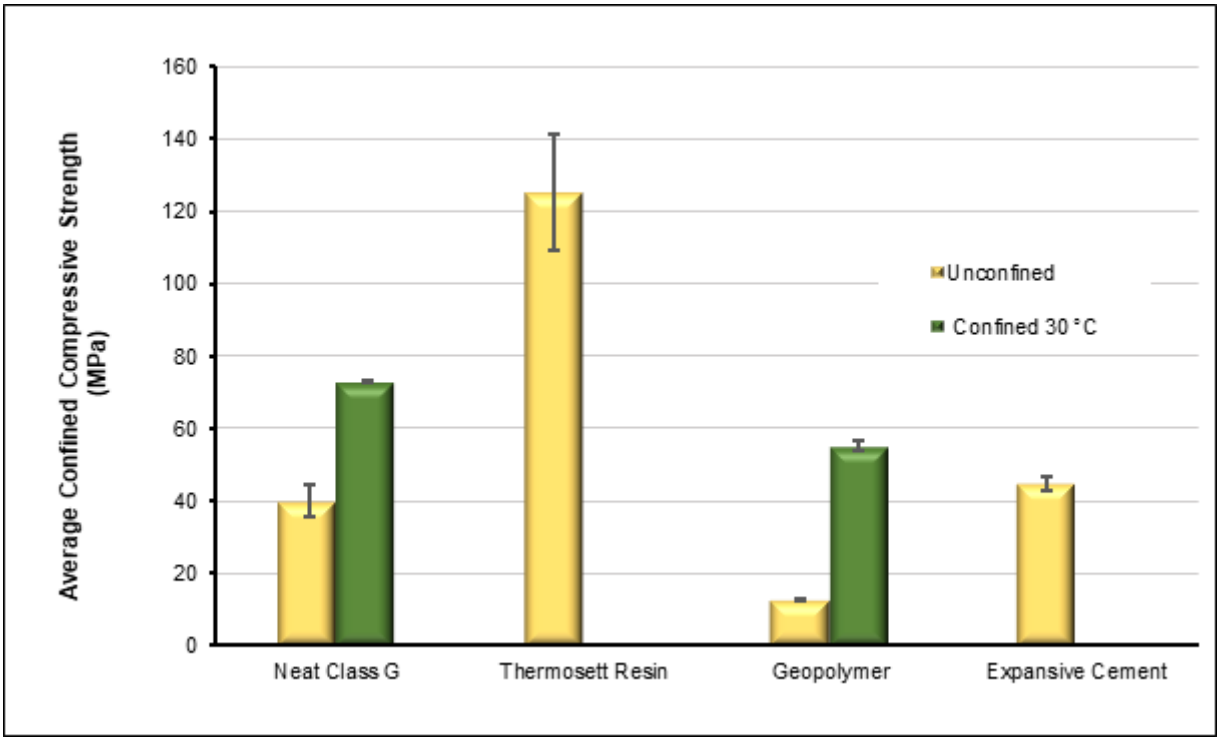


**Fig. 11—Effect of confining pressure on the average confined compressive strength of selected zonal isolation materials.**

**Cohesion and Internal Friction Angle.** Cohesion provides a measure of the inherent shear strength of a material. It is the attraction between particles based on the cementation among the particles of the material (Jönsson et al. 2005; Sujit 2015). Friction angle measures a material's resistance to the propagation of formed cracks; it is a complex function of many variables such as grain particle size, material structure, chemical composition, and porosity (Fjaer et al. 2008). Therond et al. (2017) conducted sensitivity analysis of various mechanical properties including friction angle on the integrity of the cement sheath, using a cement integrity model that includes a cement hydration process. The results indicate that increasing the friction angle of the materials decreases the risk of cement sheath damage. Increasing either cohesion or the internal friction angle of cement decreases the developed plastic strain in the cement exponentially

(Heidarian et al. 2015). A series of Mohr circles were drawn at confining pressures of $6.89 \times 10^{-3}$, 6.89, and 17.2 MPa for each material and used to acquire the shear strength envelope and the Mohr-Coulomb parameters. Cohesion was determined from the intercept of the Mohr-Coulomb failure line on the shear axis. The friction angle was determined from the coefficient of internal friction, which is estimated from the slope of the failure line. The relationship between the friction angle and coefficient of friction is expressed as follows:

$$\tan \varnothing = \mu, \quad (1)$$

where Ø is the friction angle and $\mu$ is the coefficient of friction. **Fig. 12** presents the Mohr circles describing the shear strength envelope for geopolymer and neat G cement at 30°C. The results show that geopolymer has a cohesive strength of 11.8 MPa and a coefficient of internal friction of 0.204. In contrast, neat G cement has a cohesive strength of 7 MPa and a coefficient of internal friction of 0.5417. According to the Mohr-Coulomb criterion, the shear strength of geopolymer and neat G cement can then be expressed as Eqs. 2 and 3. It can be seen that neat G cement possess a higher shear strength than geopolymer at 30°C:

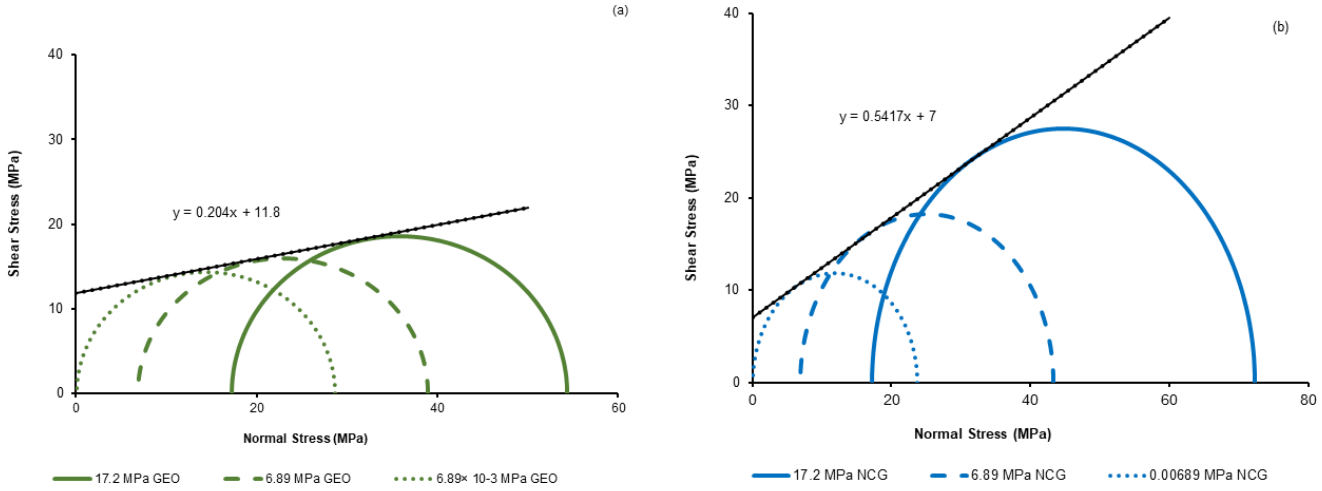


**Fig. 12—Shear strength envelope of zonal isolation materials at confining pressures $6.89 \times 10^{-3}$, 6.89, and 17.2 MPa at 30°C: (a) geopolymer and (b) neat G cement.**

$$\tau = 0.204\sigma + 11, \quad (2)$$

$$\tau = 0.5417\sigma + 7. \quad (3)$$

It should be noted that the evaluation of cohesion and friction angle for thermosetting resin may be devoid of meaning because resins are polymers, not granular materials. However, it is estimated here for the purpose of comparison. The Mohr-Coulomb parameters for thermosetting resin and expansive cement could not be estimated at 30°C because they did not fail within the maximum loading limits of the experiment. **Fig. 13** shows the shear strength envelope for the zonal isolation materials at 90°C. At 90°C, the cohesion and coefficient of internal friction of geopolymer are 7.5 MPa and 0.12, respectively. Neat G cement has a cohesive strength of 13.6 MPa and a coefficient of internal friction of 0.26. For thermosetting resin, the cohesion and coefficient of friction are 8.5 MPa and 0.17, while for expansive cement, the cohesive strength is 12.5 MPa and the coefficient of friction is 0.33. The shear strength of geopolymer, neat G cement, thermosetting resin, and expansive cement can then be expressed as Eqs. 4 through 7, respectively, according to the Mohr-Coulomb criterion:

$$\tau = 0.12\sigma + 7.5, \quad (4)$$

$$\tau = 0.26\sigma + 13.6, \quad (5)$$

$$\tau = 0.17\sigma + 8.5, \quad (6)$$

$$\tau = 0.33\sigma + 12.5. \quad (7)$$

**Table 1** presents a summary of the cohesion and friction angle of the materials at 30 and 90°C. The results show that at 90°C, expansive cement has the highest shear strength, followed by neat G cement, thermosetting resin, and geopolymer. The low cohesive strength of geopolymer and thermosetting resins may be because of a weaker bonding at the interface between its binders and fillers compared with the bond provided by the calcium silicate hydrate (C-S-H) minerals of neat G cement and expansive cement.

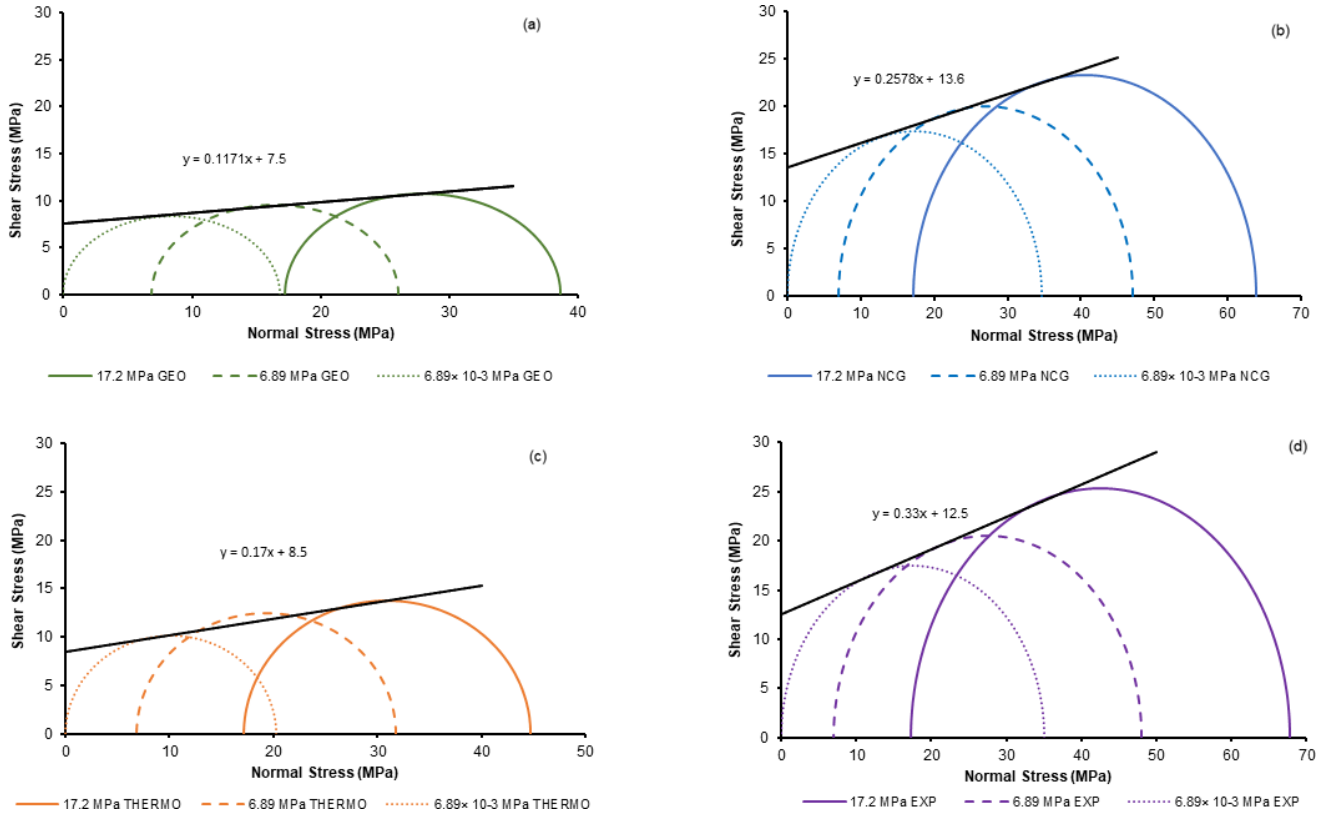


**Fig. 13—Shear strength envelope of zonal isolation materials at confining pressures 6.89 $\times 10^{-3}$, 6.89, and 17.2 MPa at 30°C: (a) geopolymer; (b) neat G cement; (c) thermosetting resin; and (d) expansive cement.**

| | 30°C | | 90°C | |
|---|---|---|---|---|
| Materials | Cohesive Strength (MPa) | Friction Angle (degrees) | Cohesive Strength (MPa) | Friction Angle (degrees) |
| Neat G | 7.0 | 28.8 | 13.6 | 14.6 |
| Geopolymer | 11.8 | 11.6 | 7.6 | 6.3 |
| Thermosetting resin | NA | NA | 8.5 | 9.6 |
| Expansive cement | NA | NA | 12.5 | 18.3 |

NA: Not available.

Table 1—Summary of the Mohr-Coulomb parameters at 30 and 90°C.

## Conclusions

Mechanical properties of the selected setting materials were examined after 7 days of curing using triaxial testing. The effects of test temperature and confining pressure were also investigated. The performance of the selected materials was compared with that of Class G cement as a reference. The results indicate that test temperature did not significantly influence Young's modulus of the materials except for thermosetting resin. It was found that an increase in test temperature leads to an increase in the Poisson's ratio of all the zonal isolation materials. When the test temperature was increased, the compressive strength of the materials decreased; all the selected materials appeared to be weaker at 90°C. There was no significant effect of confining pressure on the Young's modulus of all the zonal isolation materials. However, the compressive strength of the materials was sensitive to confining pressure. An increase in test temperature leads to a decrease of friction angle for both neat G and geopolymer. This decrease may imply a lower resistance to crack propagation in the specimen, which is consistent with the lower compressive strength of the materials at 90°C. Well operating conditions vary from well to well; therefore, the mechanical properties of the barrier materials used in each well should be tailored to fit each well's unique conditions. Compared with the neat G cement, geopolymer and thermosetting resin possess desirable mechanical properties such as a low Young's modulus and high Poisson's ratio at low and elevated temperatures. This indicates that both materials may possess adequate zonal isolation capabilities in low and elevated well environments. At both 30 and 90°C, expansive cement retained a high confined compressive strength; therefore, it may be preferred in well applications where a high compressive strength is crucial. At both 30 and 90°C, expansive cement and neat G cement showed high confined compressive strength; therefore, both zonal isolation materials should be considered in low and elevated-temperature applications where a material with a high compressive strength is preferred. Because of the difference in the chemistry of thermosetting resin, standards developed for testing the mechanical properties of cementitious materials may not reflect the true mechanical properties of thermosetting resin.

## Acknowledgments

The authors would like to thank Research Council of Norway (RCN) and NORCE for financially funding the project "#308767—Fluid migration modeling and treatment project." The authors would also like to thank RCN, TOTAL, AkerBP and ConocoPhillips for their support through the SafeRock project (#319014—New Cementitious Material for Oil Well Cementing Applications—SafeRock). Special thanks go to Halliburton, WellCem AS, and Schlumberger for provision of technical advises and chemicals. We appreciate Reidar Inge Korsnes and Emin Ahmadov for their contributions in the laboratory assistance in performing the experiments. Special thanks go to Mohammadreza Kamali for sharing his results and consultancy.

## References

Adjei, S., Elkatatny, S., Aggrey, W. N. et al. 2021. Geopolymer as the Future Oil-Well Cement: A Review. *J Pet Sci Eng* **208**: 109485. https://doi.org/10.1016/j.petrol.2021.109485.

Al-Ansari, A. A., Al-Refai, I. M., Al-Beshri, M. H. et al. 2015. Thermal Activated Resin to Avoid Pressure Build-up in Casing-Casing Annulus (CCA). Paper presented at the SPE Offshore Europe Conference and Exhibition, Aberdeen, Scotland, UK, 8–11 September. SPE-175425-MS. https://doi.org/10.2118/175425-MS.

API RP 10B-2. 2013. *Recommended Practice for Testing Well Cements*. Washington, DC: American Petroleum Institut.

API TR 10TR7. 2017. *Mechanical Behavior of Cement*. Washington, DC: American Petroleum Institute.

ASTM. 2001. *ASTM C150-07: Standard Specification for Portland Cement*. West Conshohocken, Pennsylvania, USA: ASTM International.

ASTM. 2012. *ASTM-C39: Standard Test Method for Compressive Strength of Cylindrical Concrete Specimens*. West Conshohocken, Pennsylvania, USA: ASTM.

Bagheri, M., Shariatipour, S. M., and Ganjian, E. 2018. A Review of Oil Well Cement Alteration in CO2-Rich Environments. *Constr Build Mater* **186**: 946–968. https://doi.org/10.1016/j.conbuildmat.2018.07.250.

Beharie, C., Francis, S., and Øvestad, K. H. 2015. Resin: An Alternative Barrier Solution Material. Paper presented at the SPE Bergen One Day Seminar, Bergen, Norway, 22 April. SPE-173852-MS. https://doi.org/10.2118/173852-MS.

Bois, A.-P., Garnier, A., Galdiolo, G. et al. 2012. Use of a Mechanistic Model To Forecast Cement-Sheath Integrity. *SPE Drill & Compl* **27** (2): 303–314. SPE-139668-PA. https://doi.org/10.2118/139668-PA.

Bois, A.-P.-P., Garnier, A., Rodot, F. et al. 2011. How To Prevent Loss of Zonal Isolation Through a Comprehensive Analysis of Microannulus Formation. *SPE Drill & Compl* **26** (1): 13–31. SPE-124719-PA. https://doi.org/10.2118/124719-PA.

Boukhelifa, L., Moroni, N., James, S. G. et al. 2004. Evaluation of Cement Systems for Oil and Gas Well Zonal Isolation in a Full-Scale Annular Geometry. Paper presented at the IADC/SPE Drilling Conference, Dallas, Texas, 2–4 March. SPE-87195-MS. https://doi.org/10.2118/87195-MS.

Chen, J. and Xu, C. 2018. A Study of the Shear Behavior of A Portland Cement Grout with the Triaxial Test. *Constr Build Mater* **176**: 81–88. https://doi.org/10.1016/j.conbuildmat.2018.04.189.

Davies, R. J., Almond, S., Ward, R. S. et al. 2014. Oil and Gas Wells and Their Integrity: Implications for Shale and Unconventional Resource Exploitation. *Mar Pet Geol* **56**: 239–254. ;. https://doi.org/10.1016/j.marpetgeo.2014.03.001.

Davis, J. E. 2017. Using a Resin-Only Solution to Complete a Permanent Abandonment Operation in the Gulf of Mexico. Paper presented at the SPE Offshore Europe Conference & Exhibition, Aberdeen, United Kingdom, 5–8 September. SPE-186113-MS. https://doi.org/10.2118/186113-MS.

De Andrade, J., Sangesland, S., Skorpa, R. et al. 2016. Experimental Laboratory Setup for Visualization and Quantification of Cement-Sheath Integrity. *SPE Drill & Compl* **31** (4): 317–326. SPE-173871-PA. https://doi.org/10.2118/173871-PA.

Fjaer, E., Holt, R. M., Horsrud, P. et al. 2008. *Petroleum Related Rock Mechanics*. Amsterdam, The Netherlands: Elsevier.

Geiker, M. and Knudsen, T. 1982. Chemical Shrinkage of Portland Cement Pastes. *Cem Concr Res* **12** (5): 603–610. https://doi.org/10.1016/0008-8846(82)90021-7.

Heidarian, M., Jalalifar, H., Schaffie, M. et al. 2015. Effect of Mechanical and Geometrical Properties of Cement on Wellbore Stability Using 3-D Analysis. *Walailak J Sci Technol* **12** (8): 721–731.

Jafariesfad, N., Geiker, M. R., Gong, Y. et al. 2017a. Cement Sheath Modification Using Nanomaterials for Long-Term Zonal Isolation of Oil Wells: Review. *J Pet Sci Eng* **156**: 662–672. https://doi.org/10.1016/j.petrol.2017.06.047.

Jafariesfad, N., Geiker, M. R., and Skalle, P. 2017b. Nanosized Magnesium Oxide With Engineered Expansive Property for Enhanced Cement-System Performance. *SPE J.* **22** (5): 1681–1689. SPE-180038-PA. https://doi.org/10.2118/180038-PA.

Jafariesfad, N., Khalifeh, M., Skalle, P. et al. 2017c. Nanorubber-Modified Cement System for Oil and Gas Well Cementing Application. *J Nat Gas Sci Eng* **47**: 91–100. https://doi.org/10.1016/j.jngse.2017.10.002.

Jönsson, B., Nonat, A., Labbez, C. et al. 2005. Controlling the Cohesion of Cement Paste. *Langmuir* **21** (20): 9211–9221. https://doi.org/10.1021/la051048z.

Kamali, M., Khalifeh, M., Eid, E. et al. 2021a. Experimental Study of Hydraulic Sealability and Shear Bond Strength of Cementitious Barrier Materials. *J Energy Resour Technol* **144** (2): 023007. JERT-21-1253. https://doi.org/10.1115/1.4051269.

Kamali, M., Khalifeh, M., Saasen, A. et al. 2021b. Alternative Setting Materials for Primary Cementing and Zonal Isolation – Laboratory Evaluation of Rheological and Mechanical Properties. *J Pet Sci Eng* **201**: 108455. https://doi.org/10.1016/j.petrol.2021.108455.

Kimanzi, R., Wu, Y., Salehi, S. et al. 2020. Experimental Evaluation of Geopolymer, Nano-Modified, and Neat Class H Cement by Using Diametrically Compressive Tests. *J Energy Resour Technol* **142** (9). JERT-19-1780. https://doi.org/10.1115/1.4046702.

Khalifeh, M., Hodne, H., Korsnes, R. I. et al. 2015. Cap Rock Restoration in Plug and Abandonment Operations; Possible Utilization of Rock-Based Geopolymers for Permanent Zonal Isolation and Well Plugging. Paper presented at the International Petroleum Technology Conference, Doha, Qatar, 6–9 December. IPTC-18454-MS. https://doi.org/10.2523/IPTC-18454-MS.

Khalifeh, M. and Saasen, A. 2020. Introduction to Permanent Plug and Abandonment of Wells. In *Introduction to Permanent Plug and Abandonment of Wells*. Cham: Springer Nature. https://doi.org/10.1007/978-3-030-39970-2.

Khalifeh, M., Saasen, A., Hodne, H. et al. 2018. Geopolymers as an Alternative for Oil Well Cementing Applications: A Review of Advantages and Concerns. *J Energy Resour Technol* **140** (9). JERT_140_09_092801. https://doi.org/10.1115/1.4040192.

Kiran, R., Teodoriu, C., Dadmohammadi, Y. et al. 2017. Identification and Evaluation of Well Integrity and Causes of Failure of Well Integrity Barriers (A Review). *J Nat Gas Sci Eng* **45**: 511–526. https://doi.org/10.1016/j.jngse.2017.05.009.

Kjøller, C., Torsæter, M., Lavrov, A. et al. 2016. Novel Experimental/Numerical Approach to Evaluate the Permeability of Cement-Caprock Systems. *Int J Greenh Gas Control* **45**: 86–93. https://doi.org/10.1016/j.ijggc.2015.12.017.

Kwatia, G., Ezeakacha, C., and Salehi, S. 2017. Literature Report of Elastomer Sealing Materials and Cement Systems. *BSEE Project* **E17PC00005**: 1–78.

Lavrov, A., Todorovic, J., and Torsæter, M. 2015. Numerical Study of Tensile Thermal Stresses in a Casing-Cement-Rock System with Heterogeneities. Paper presented at the 49th US Rock Mechanics/Geomechanics Symposium, San Francisco, California, 28 June–1 July. ARMA-2015-110.

Le Roy-Delage, S., Baumgarte, C., Thiercelin, M. et al. 2000. New Cement Systems for Durable Zonal Isolation. Paper presented at the IADC/SPE Drilling Conference, New Orleans, Louisiana, 23–25 February. SPE-59132-MS. https://doi.org/10.2118/59132-MS.

Lecampion, B., Bunger, A., Kear, J. et al. 2013. Interface Debonding Driven by Fluid Injection in a Cased and Cemented Wellbore: Modeling and Experiments. *Int J Greenh Gas Con* **18**: 208–223. https://doi.org/10.1016/j.ijggc.2013.07.012.

Mo, L., Deng, M., Tang, M. et al. 2014. MgO Expansive Cement and Concrete in China: Past, Present and Future. *Cem Concr Res* **57**: 1–12. https://doi.org/10.1016/j.cemconres.2013.12.007.

Mo, L., Deng, M., and Wang, A. 2012. Effects of MgO-Based Expansive Additive on Compensating the Shrinkage of Cement Paste under Non-Wet Curing Conditions. *Cem Concr Compos* **34** (3): 377–383. https://doi.org/10.1016/j.cemconcomp.2011.11.018.

Nelson, E. B. and Guillot, D. 2006. *Well Cementing*, 2nd Edition, Vol. 77478, 258–263. Sugar Land, Texas, USA: Schlumberger.

NORSOK D-010. 2021. *D-010 Well Integrity in Drilling and Well Operations*, Vol. 5. Norway: Standards Norway.

Norwegian Petroleum Directorate. 2021. Factpages. Retrieved From. https://factpages.npd.no/nb-no/wellbore/statistics/entryyear.

Saito, M., Kawamura, M., and Arakawa, S. 1991. Role of Aggregate in the Shrinkage of Ordinary Portland and Expansive Cement Concrete. *Cem Concr Compos* **13** (2): 115–121. https://doi.org/10.1016/0958-9465(91)90006-4.

Salehi, S., Khattak, M. J., Ali, N. et al. 2018. Study and Use of Geopolymer Mixtures for Oil and Gas Well Cementing Applications. *J Energy Resour Technol* **140** (1). JERT-17-1290. https://doi.org/10.1115/1.4037713.

Sasaki, T., Soga, K., and Abuhaikal, M. 2018. Water Absorption and Shrinkage Behaviour of Early-Age Cement in Wellbore Annulus. *J Pet Sci Eng* **169**: 205–219. https://doi.org/10.1016/j.petrol.2018.05.065.

Shen, W., Cao, L., Li, Q. et al. 2015. Quantifying CO2 Emissions from China's Cement Industry. *Renew Sustain Energy Rev* **50**: 1004–1012. https://doi.org/10.1016/j.rser.2015.05.031.

Sherir, M. A. A., Hossain, K. M. A., and Lachemi, M. 2017. Development and Recovery of Mechanical Properties of Self-Healing Cementitious Composites with MgO Expansive Agent. *Constr Build Mater* **148**: 789–810. https://doi.org/10.1016/j.conbuildmat.2017.05.063.

Sujit, M. 2015. Assessing Cohesion, Friction Angle and Slope Instability in the Shivkhola Watershed of Darjiling Himalaya. *Int J Earth Sci* **3** (8): 1–7.

Therond, E., Bois, A.-P., Whaley, K. et al. 2017. Large-Scale Testing and Modeling for Cement Zonal Isolation in Water-Injection Wells. *SPE Drill & Compl* **32** (4): 290–300. SPE-181428-PA. https://doi.org/10.2118/181428-PA.

Thiercelin, M., Baumgarte, C., and Guillot, D. 1998. A Soil Mechanics Approach To Predict Cement Sheath Behavior. Paper presented at the SPE/ISRM Rock Mechanics in Petroleum Engineering, Trondheim, Norway, 8–10 July. SPE-47375-MS. https://doi.org/10.2118/47375-MS.

Van den Ende, D. A., De Almeida, P., and Van der Zwaag, S. 2007. Piezoelectric and Mechanical Properties of Novel Composites of PZT and a Liquid Crystalline Thermosetting Resin. *J Mater Sci* **42** (15): 6417–6425. https://doi.org/10.1007/s10853-006-1257-3.

Vignes, B. 2011. *Contribution to Well Integrity and Increased Focus on Well Barriers from a Life Cycle Aspect*., PhD dissertation, University of Stavanger, Stavanger, Normawy (August 2011).

Vrålstad, T., Saasen, A., Fjær, E. et al. 2019a. Plug & Abandonment of Offshore Wells: Ensuring Long-Term Well Integrity and Cost-Efficiency. *J Pet Sci Eng* **173**: 478–491. https://doi.org/10.1016/j.petrol.2018.10.049.

Vrålstad, T., Skorpa, R., and Werner, B. 2019b. Experimental Studies on Cement Sheath Integrity During Pressure Cycling. Paper presented at the SPE/IADC International Drilling Conference and Exhibition, The Hague, The Netherlands, 5–7 March. SPE-194171-MS. https://doi.org/10.2118/194171-MS.

Wu, Y. and Salehi, S. 2020. A Numerical and Experimental Study on Cement Integrity Based on A Novel Method. Paper presented at the 54th US Rock Mechanics/Geomechanics Symposium.

Zhang, M. and Bachu, S. 2011. Review of Integrity of Existing Wells in Relation to CO2 Geological Storage: What Do We Know? *Int J Greenh Gas Control* **5** (4): 826–840. https://doi.org/10.1016/j.ijggc.2010.11.006.

Zheng, Y., Xu, B., Pu, J. et al. 2017. Mechanical Behaviors of Cement Systems in Different Conditions. *Nat Gas Ind B.* **4** (3): 212–216. https://doi.org/10.1016/j.ngib.2017.07.022.